

Scanning tunneling microscopy (STM)  
of a diamond-turned surface and a grating replica

R. A. Dragoset and T. V. Vorburger  
National Bureau of Standards  
Gaithersburg, MD 20899

Abstract

The technique of scanning tunneling microscopy has been applied to topographic mapping of two optical surfaces -- a ruled grating replica and a diamond-turned gold mirror. By taking measurements with both a scanning tunneling microscope and a conventional stylus instrument, we have compared profiles and power spectral density (PSD) functions calculated from the profiles of a grating replica. Furthermore, surface structure was observed and PSD's were calculated for a diamond-turned surface measured with a STM. No structure was detected by the stylus instrument due to the spacing of the grooves on the diamond-turned sample. These measurements yield information necessary to gaining a better understanding of the diamond-turning process.

Introduction

The scanning tunneling microscope has recently been shown to have extremely high resolution in measuring topographic maps of conductor [1] and semiconductor [2] surfaces. Its operating principle is similar to that of the topografiner, developed by Young et al. [3], a surface mapping instrument that employed a tip in the field emitting mode (10 - 20 nm from the surface) that was raster scanned across a conducting surface. The vertical position of the tip was adjusted to maintain a constant field emission current, thus mapping out surface topographs as the tip was scanned over the surface area. The STM, developed by Binnig and Rohrer [4], uses a similar scanning technique with improved vibration isolation and design changes allowing the tip to be much closer to the surface (1 - 2 nm) and to operate in the tunneling mode. The STM has been shown to have atomic resolution when applied to studies of single crystals and other surfaces of interest to surface scientists. We have used a STM for the different purpose of measuring the topography of two optical surfaces -- a gold, ruled grating replica and a polycrystalline, diamond-turned gold sample; and we have studied the resulting power spectral density (PSD) functions for these surfaces. These two surfaces were chosen primarily to demonstrate the benefit of using a scanning tunneling microscope to detect the perfection of optical surfaces with higher sensitivity and resolution than had been previously obtainable by other techniques such as the stylus technique and optical scattering.

Description of the STM

The STM used for these measurements is nearly identical to that of Binnig and Rohrer [4]. The fine motion of the tip (<3  $\mu\text{m}$  in each of three orthogonal directions) is controlled by a tripod of piezoelectric sticks. The x and y sticks provide the raster scanning of the tip over the surface; and the z stick, adjusted by means of servo-controlled feedback, maintains a constant tunneling current between the voltage-biased sample and the tip, thus maintaining a constant tip-to-surface distance. The sample is brought within the range of the tip by means of a piezoelectric/electrostatic clamping device known as a walker, or "louse," as described by Binnig and Rohrer [4]. The tip/tripod and the sample/walker devices are both mounted on a quartz plate that is held in a magnetically-damped, double spring suspension system for vibration isolation. For these measurements, this apparatus was mounted in an ion-pumped, glass bell jar vacuum chamber that attained a vacuum of  $\sim 2 \times 10^{-8}$  torr.

The ability of the STM to attain high vertical resolution is dependent on the exponential behavior of the tunneling current as a function of the gap distance with constant bias voltage [5]. It is believed that nearly all of the tunneling current (typically  $\sim 1$  nA) passes through the last few atoms on the end of the tip. For a clean surface with a high work function, such as gold, the tunneling probability decreases by an order of magnitude for a 0.1 nm increase in the tunneling gap. Therefore, when examining extremely flat areas of surfaces, the shape of the tip beyond the last few atoms has no effect [4]. However, since the grating replica was known to have relatively large surface structure with high slopes, we developed a tip etching process [6] that reproducibly forms tips well characterized to  $<0.5$   $\mu\text{m}$  radius and generally produces tips with  $<0.1$   $\mu\text{m}$  radius. Since the shapes of the tips were generally not known beyond the  $\sim 0.1$   $\mu\text{m}$  radius, better tip characterization would be required for any future work involving surface topographies with structures such as that of the grating replica.

### Ruled grating replica

The Au film grating replica (described in Ref. 6) was manufactured as a dimensional calibration standard for scanning electron microscopes, and can be approximated by raised lines separated by flat areas. The single profile (a) and the topographic map (b) in Fig. 1 demonstrate the capabilities of a conventional stylus instrument [6-8] and a STM in measuring surface structure. The STM topographic map has been corrected for nonlinearity in both lateral dimensions. The area covered by this map is much larger than is customary for a STM. The difference between the average surface rms roughness (calculated relative to "best fit" straight lines for single profiles) determined from the STM data (5.4 nm) and that determined from the stylus instrument data (4.3 nm) can be attributed to a better lateral resolution of the STM tunneling tip than the stylus tip.

The PSD's of the grating replica (Fig. 2) were calculated [9] using several profiles as measured by the stylus instrument and by the STM. These were one-dimensional PSD's, calculated along the profiling direction which was close to the direction of maximum roughness. The PSD's for both measurement techniques show the primary periodicity of  $0.46 \mu\text{m}$  (spatial frequency  $\sim 2.2 \mu\text{m}^{-1}$ ) and two higher harmonics. The amplitude of the STM-PSD is greater in the higher frequency region than the amplitude of the stylus-PSD. This may be attributed to the sensitivity of the STM to smaller surface structure and the ability to attain more information in the "valleys" of the grating replica. Based on information about the surface structure (described above and in Ref. 6), the grating replica should have a positive skewness. Skewness, a calculated surface parameter, is a measure of the symmetry of a profile about the mean line. As described by Vorburger and Hembree [9], the skewness of the grating replica profiles calculated from the STM data is positive, whereas the skewness calculated from stylus measurements is negative. That is, the valleys in the stylus profile are sharper than the peaks. This suggests that the stylus tip is not capable of fully resolving the valleys and supports the idea that the STM measurement yields a better representation of the surface of the grating replica than does the stylus instrument. However, the higher amplitude of the STM-PSD could also be attributed to a jagged tunneling tip that produces higher frequency structure in the topographic map, which is actually a convolution of surface geometry and tip geometry.

The non-contacting probe of the STM has distinct advantages over the contacting diamond tip used in the stylus instrument, since the end of the tip and the measured surface should exhibit no wear or damage. However, in order to take full advantage of this aspect of the STM when mapping surface structure on this scale, better tip characterization is essential.

### Diamond-turned gold mirror

The STM was also used to measure surface structure of a polycrystalline diamond-turned Au sample with  $0.1 \mu\text{m}$  spacings between adjacent machined cuts (described in Ref. 6). The surface structure measured by the STM is represented with three different magnifications in the topographic maps of Figs. 3-5. It was necessary to correct the large area map ( $1.6 \mu\text{m} \times 1.6 \mu\text{m}$  - Fig. 3) for piezo nonlinearity in the lateral dimensions. Correction for piezo nonlinearity was unnecessary for the small area maps (Figs. 4 and 5), but the scan direction was changed by  $30^\circ$  for these two maps in order to scan in a direction perpendicular to the tool markings. Figure 4 shows a scanned area ( $0.6 \mu\text{m} \times 0.3 \mu\text{m}$ ) of the diamond-turned sample that was recorded with a high density of data points (401) in each scan and a relatively few number of scans (20). However, for displaying the information in Fig. 4, the data points have been connected between adjacent scan lines and not within each scan line; this process "fills in" the surface and structure is more easily observed. As observed in these topographic maps, the spacing between adjacent cuts is irregular (Figs. 3 and 4), which may be caused by a non-uniform tool feed or variation in the depth of cut [6]. Furthermore, there is considerable structure detected within a single pass of the tool (Figs. 4 and 5), which may be attributed to a tool signature that is changing during the cutting process or to chatter of the machine tool [6].

The PSD's of the diamond-turned sample (Fig. 6) were calculated from the data in Figs. 3 and 4. The PSD's were calculated after interpolation of the data was made so that the number of data points was increased to a power of two. For the  $0.6 \mu\text{m}$  scans, the number of data points was interpolated from 401 to 512; and for the  $1.6 \mu\text{m}$  scans, the number of data points was interpolated from 201 to 256. This procedure tends to smooth out the high frequency structure in the surface profile. The PSD of the data in Fig. 5 showed no interesting structure due to the inability to obtain periodic information in such a small scan area. (The three peaks are not equally spaced and this data is thought to be produced by only one, or maybe two, passes of the cutting tool.) The PSD calculated from the data in Fig. 3 shows a strong peak at  $8.6 \mu\text{m}^{-1}$  which corresponds to a surface periodicity of  $0.12 \mu\text{m}$ . However, the scan direction was  $30^\circ$  off from scanning perpendicular to the tool cuts. After applying a correction factor ( $\cos 30^\circ$ ), the spacing is found to be  $0.1 \mu\text{m}$  which compares favorably with the machining process information.

The PSD calculated from the data in Fig. 4 shows two relatively strong peaks at  $11.6 \mu\text{m}^{-1}$  and  $18.3 \mu\text{m}^{-1}$  which correspond to periodicities of  $0.086 \mu\text{m}$  and  $0.055 \mu\text{m}$ , respectively. The difference between the low frequency periodicities in the PSD's is probably due to some short term variation in the machining process as observed in the variations seen in Fig. 4. The scan range of  $0.6 \mu\text{m}$  at this location on the surface was not sufficient to determine accurately the fundamental frequency of the periodic surface structure. However, the  $0.6 \mu\text{m}$  scan produced a higher amplitude of high frequency information in the PSD in comparison to that calculated from the  $1.6 \mu\text{m}$  scan data of Fig. 3. We have no ready explanation for the difference between the two PSD curves above a spatial frequency of  $15 \mu\text{m}^{-1}$ . Perhaps it was due to the fact that different areas on the surface were sampled by the two maps coupled with the possibility that the  $0.6 \mu\text{m} \times 0.3 \mu\text{m}$  area may have had more short wavelength structure. Another possibility is that the instrumental resolution may have changed between the times that the two maps were recorded.

### Conclusions

We have shown the capability of the scanning tunneling microscope to measure surface topography with considerably higher resolution than that possible with a conventional stylus instrument. Furthermore, we have calculated power spectral densities for these two optical surfaces in order to determine the surface periodicities and to compare different scanning methods. We conclude that the STM is a useful instrument for making these types of surface measurements, and could be applied particularly to the examination of UV and x-ray mirrors. The resolution necessary for optical surface characterization is not as great as that necessary for a surface science study and is relatively easy to obtain. Finally, a larger mapping area would be helpful for future studies involving optical surfaces.

### Acknowledgments

We want to thank R. D. Young, H. P. Layer, S. R. Mielczarek, E. C. Teague, and R. J. Celotta for their work and input on the STM project, C. H. W. Glauque and F. E. Scire for the stylus measurements, and R. L. Rhorer and E. Baumgartner of Los Alamos National Laboratory for fabricating the diamond-turned specimen.

### References

1. G. Binnig, H. Rohrer, Ch. Gerber, and E. Weibel, Surf. Sci. 131, L379 (1983).
2. G. Binnig, H. Rohrer, Ch. Gerber, and E. Weibel, Phys. Rev. Lett. 50, 120 (1983).
3. R. Young, J. Ward, and F. Scire, Rev. Sci. Instrum. 43, 999 (1972).
4. G. Binnig and H. Rohrer, Surf. Sci. 126, 236 (1983).
5. Theoretical: J. G. Simmons, J. Appl. Phys. 34, 1793 (1963). Experimental: R. D. Young, J. Ward, and F. Scire, Phys. Rev. Lett. 27, 922 (1971); and E. C. Teague, J. Res. NBS 91, 171 (1986).
6. R. A. Dragoset, R. D. Young, H. P. Layer, S. R. Mielczarek, E. C. Teague, and R. J. Celotta, Opt. Lett. 11, 560 (1986).
7. The stylus instrument used for measurements was a digitized Talystep. A description of the instrument can be found in E. L. Church, T. V. Vorburger, and J. C. Wyant, Opt. Eng. 24, 388 (1985) and a similar instrument is described in Ref. 8. The commercial part of the instrument is identified in this paper to specify experimental procedures. In no case does this identification imply recommendation or endorsement by the National Bureau of Standards, nor does it imply that the equipment identified is necessarily the best available for the purpose.
8. J. M. Bennett and J. H. Dancy, Appl. Opt. 20, 1785 (1981).
9. T. V. Vorburger and G. G. Hembree, "Characterization of surface topography," in Methods of Surface Characterization, Vol. 3 (Plenum, 1986) (in press).

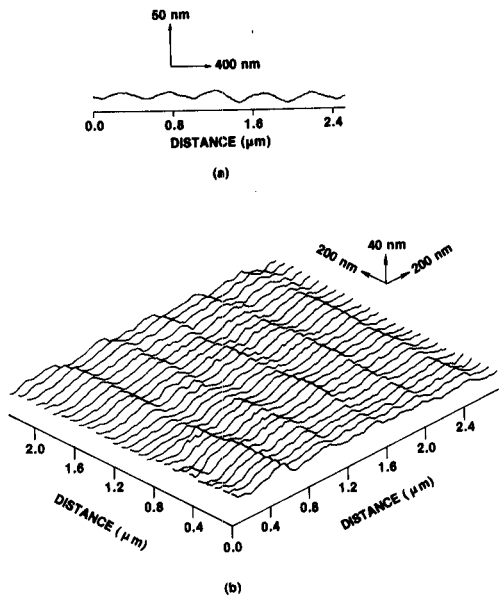


Figure 1. (a) Single profile of a grating replica measured by a conventional stylus instrument. The measured surface rms roughness is  $\sim 4.3$  nm. (b) STM topographic map of a grating replica. The measured surface rms roughness is  $\sim 5.4$  nm. (taken from Ref. 6)

COMPARISON OF PSDs OF STM AND STYLUS PROFILES OF  $0.46 \mu\text{m}$  PERIOD GRATING

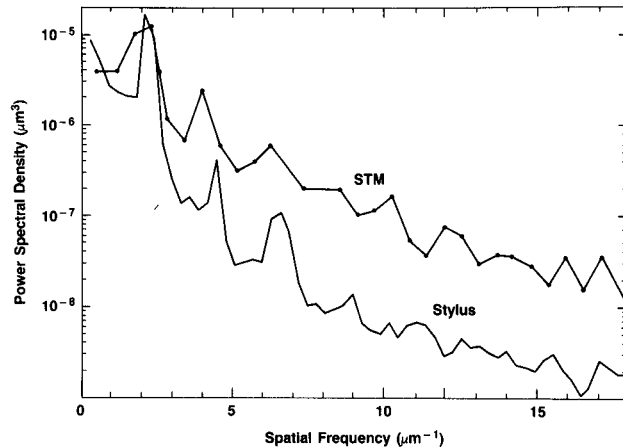


Figure 2. Power spectral density functions calculated from stylus and STM profiles of the grating replica. Each curve is an average of PSD results for several profiles. The stylus PSD was calculated from three profiles each having 4000 digitized points and a length of  $13.4 \mu\text{m}$ . The PSD measured by STM was calculated from the 27 profiles making up the map of Fig. 1(b), each of these containing 101 points and having a length of  $2.75 \mu\text{m}$ . (taken from Ref. 9)

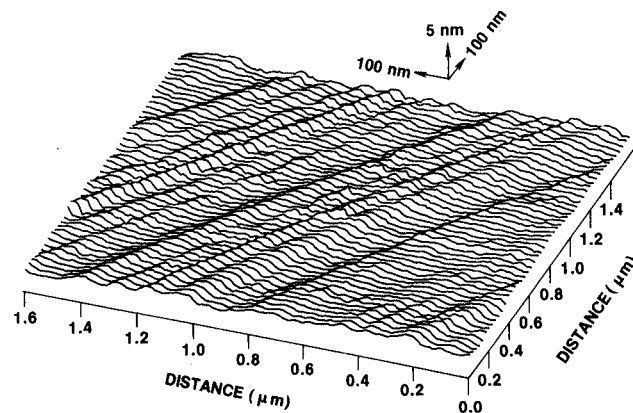


Figure 3. Large-area topographic map of a diamond-turned Au mirror. The surface rms roughness is  $\sim 0.6$  nm. (taken from Ref. 6)

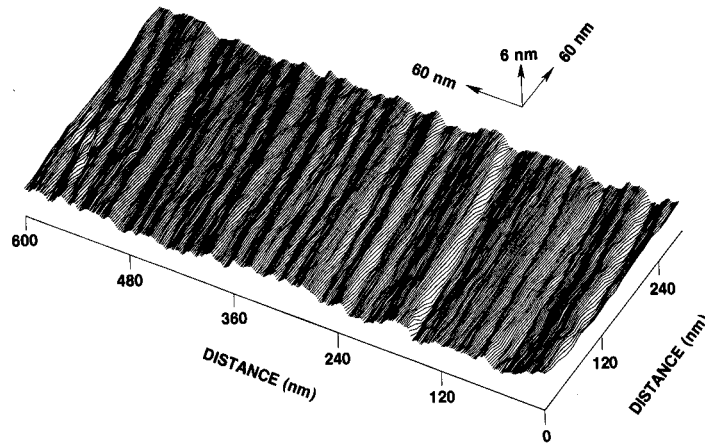


Figure 4. High-density topographic map of a diamond-turned Au mirror. The original data is composed of 20 scan lines with 401 data points per scan. However, for presentation, the data points have been connected between adjacent scan lines as opposed to connecting data points within one scan, as in the previous maps. This technique "fills in" the surface and consequently surface structure is more easily observed.

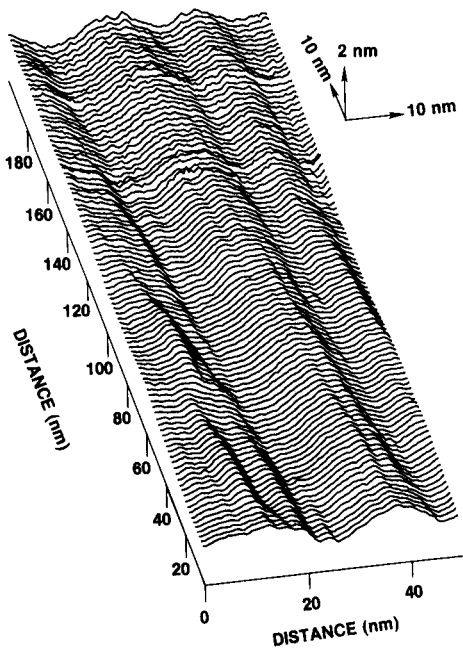


Figure 5. Surface structure of a diamond-turned Au mirror within one pass of the cutting tool. The surface rms roughness is  $\sim 0.4$  nm. (taken from Ref. 6)

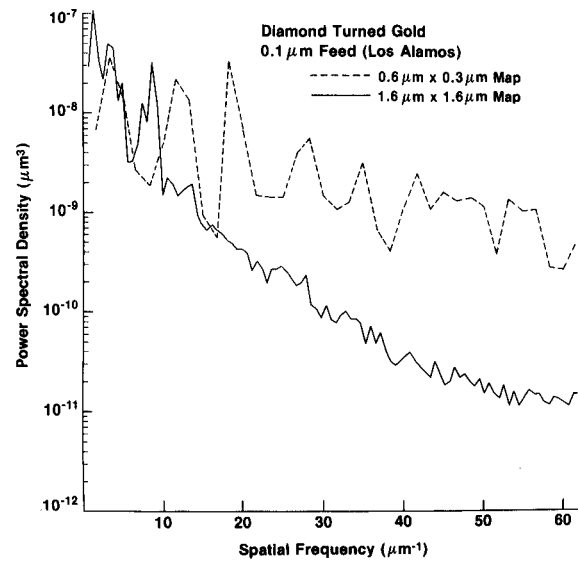


Figure 6. Power spectral density functions calculated from single profiles of the STM topographic maps (shown in Figs. 3 & 4) of the diamond-turned Au mirror. Each curve is an average of PSD results for all of the profiles in each map. In Fig. 3 there are 201 data points per profile of length  $1.6 \mu\text{m}$ , and in Fig. 4 there are 401 data points per profile of length  $600$  nm.